J Appl Electrochem (2008) 38:897–906
DOI 10.1007/s10800-008-9492-8

ORIGINAL PAPER

SFG and DFG investigation of Au(111), Au(210), polycrystalline Au, Au–Cu and Au–Ag–Cu electrodes in contact with aqueous solutions containing KCN and 4-cyanopyridine

Benedetto Bozzini · Bertrand Busson · Claudio Mele · Abderrahmane Tadjeddine

Received: 25 July 2007 / Revised: 8 January 2008 / Accepted: 18 January 2008 / Published online: 9 February 2008

Abstract We report on potential-dependent in situ SFG and DFG spectroscopy carried out at Au(111), Au(210), polycrystalline Au, Au–Cu and Au–Ag–Cu electrodes in contact with aqueous solutions containing CN^- and 4-cyanopyridine (4CP). Spectroelectrochemical work was complemented by cyclic voltammetry. The chief stress has been placed on systematising and quantifying the interaction between 4CP and CN^- and the attending effects on the vibrational and electronic structures of the interface. The voltammetric behaviour of the investigated electrodes, modified by the addition of 4CP to the CN^- electrolyte, denote changes in the CN^- adsorption characteristics and effects of the adsorbed CN^- layer on the electrodic reactivity of 4CP. The differences among the investigated electrodes can be explained in terms of their respective degrees of atomic packing or with alloying effects on the stability of adsorbed CN^-. The potential-dependent spectra have been analysed quantitatively with a model for the second order non linear susceptibility accounting for vibrational and electronic effects. The spectral changes induced by addition of 4CP denote interaction of the aromatic with the electrode through the CN^- monolayer. The non-resonant contribution yields information on the effects of 4CP on the fine structure of the bound electron density of states.

Keywords SFG · DFG · Cyanide · 4-cyanopyridine · Au(111) · Au(210) · Au–Cu · Au–Ag–Cu

B. Bozzini · C. Mele (✉)
Dipartimento di Ingegneria dell'Innovazione,
Università di Lecce, v. Monteroni, 73100 Lecce, Italy
e-mail: claudio.mele@unile.it

B. Busson
CLIO-LCP, Université Paris-Sud, 91405 Orsay Cedex, France

A. Tadjeddine
UDIL-CNRS, Bat. 201, centre Universitaire Paris-Sud, BP 34,
91898 Orsay Cedex, France

1 Introduction

The electrochemical behaviour of 4-cyanopyridine (4CP) has been intensively studied in a close-knit series of papers, which have addressed the issues of adsorption, reorientation and reactivity [1–13]. The pioneering voltammetric study of 4CP at Au(111) [1] essentially disclosed the potential range of adsorption and highlighted a potential-dependent reorientation process. The electrodic study of 4CP has been furthered by spectroelectrochemical methods. FTIR studies of 4CP on Au(111) [2, 3] have disclosed: (i) the formation of 4-cyanopyridinium cations at cathodic potentials exceeding –1 V_{SCE}; (ii) the hydrolysation of 4CP to isonicotinamide at potentials more anodic than 50 mV_{SCE}; (iii) the existence of an oxidation reaction at anodic potentials exceeding 0.6 V_{SCE}. Studies on Au(111) and Au(100) [4, 5] have shown that the reactivity of 4CP can be rationalised in terms of successive reactions which are driven by a sequence of polarisation steps: 4CP adsorbed vertically through the heteroaromatic N can undergo protonation at high cathodic potentials, if the electrode with an adsorbed protonated species is polarised to more anodic values, the adsorbate can hydrolyse and eventually transform into isonicotinamide via a tautomeric equilibrium. Concerning reorientation, the following conclusions have been proposed. On the basis of voltammetric work [1] it is suggested that vertical adsorption through CN at $V > 0.3$ V_{SCE}. FT-IR data [2] conclude that a

flat-to-vertical transition takes place at −0.15 V_{SCE} with vertical adsorption through the heteroaromatic N. A detailed orientation analysis has been carried out by SFG on Au(111) [4–6], the following sequence was suggested: in the range: −1.0 to $-0.6V_{Ag/AgCl}$ vertical adsorption through the heteroaromatic N; −0.5 to +0.1 $V_{Ag/AgCl}$ flat orientation; more positive than +0.2 V vertical adsorption through the nitrile. The electrochemical reduction of 4CP at Ag electrodes has been studied by SERS [7–9]; several reaction paths have been conjectured on the basis of the different adsorbed reaction products identified spectro-electrochemically. The chief findings are the following: (i) the release of CN^- has been highlighted for potentials more cathodic than −1.25 V_{SCE} [7]; (ii) the formation of 4-cyanopyridinium cations [8]; (iii) the existence of two alternative electroreductive reaction paths as a function of 4CP concentration: the formation of CN^- and pyridinium at low concentrations and a bimolecular reaction yielding azo-4-methylpyridine at high concentrations [9].

In previous papers [10–13] we have reported on the effects of 4CP as an additive for processes relevant to both cathodic and anodic metal electrochemistry in aqueous solutions. Notwithstanding its electrodic reactivity, this molecule seems a promising additive for Au, Au alloy and Cu electroplating and for the protection of Ag in Cl^--containing environments. In particular, on the basis of electrodeposition experiments, in situ FT-IR and SERS and ex situ XRD studies, we have stressed the surface chemical and structural effects of the coadsorption of 4CP and CN^- [10, 11]. Coadsorption of organics with ligands released during the metal reduction process was shown to have a major impact on electrodeposition kinetics, electrode morphology evolution and texturing. In particular, an understanding of the specific effects of the interaction of different moieties with specific crystal faces is strongly required for the design of innovative and environmentally acceptable metal finishing processes. Even though the use of organics in cyanide plating baths is common industrial practice, a very limited amount of published work is available specifically addressing the electrodic coadsorption of these species with CN^-, both in the double-layer charging region and during plating.

Some of the systems which have been studied and are relevant to metal electrochemistry are listed below. A voltammetric assessment of the desorption of hexadecil-thiolate from Au by immersion in KCN aqueous solutions has been reported [14]. The coadsorption of CN^-, OH^- and SO_4^{2-} on Pt(111) by in situ FT-IR has been investigated [15]. The coadsorption of aminoacid reaction products and CN^- released by electrochemical reaction at Pt single crystals was highlighted by FT-IR [16–20]. A voltammetric and FT-IR study of the coadsorption of citrate and CN^- onto polycrystalline Au has been reported [21]. The coadsorption of benzyldimethylphenylammonium chloride and CN^- was studied during Au electrodeposition [22]. Recent work in our group has attacked the problem of the coadsorption of CN^- and cetylpyridinium chloride (CPC) onto Au(111) and Au(210) by SFG [23] and onto Ag(111) by FT-IR and SERS [24]. Two basic modes of coadsorption of CN^- and organics were found. In all cases except with CPC, partial coverage with both species is observed; with CPC an interfacial bi-layer is formed, with CN^- weakly bound to the metal bearing CP^+ on top of it; CP^+ can reorient as a function of the electrode potential.

In the present paper we report potential-dependent in situ SFG and DFG spectroscopy carried out at single crystal ((111) and (210))and polycrystalline Au and Au alloy (Au–Cu and Au–Ag–Cu) electrodes in contact with an aqueous solution containing CN^- and 4CP.

2 Experimental

The solution employed was: KCN 25 mM, 4-cyanopyridine 25 mM, $NaClO_4$ 0.1 M. Analytic grade chemicals were dissolved in ultra-pure water of resistivity 18.2 MΩ cm, obtained with a Millipore Milli-Q system. The working electrodes were single-crystal Au(111) and Au(210) and polycrystalline Au, Au–Cu (Cu 25%) and Au–Ag–Cu (Ag 10%, Cu 15%). The single crystals were discs of 3 mm diameter and 4 mm thickness, the polycrystals were discs of 10 mm diameter and 3 mm thickness. The single crystals were purchased from MaTeck Gmbh, the polycrystal were prepared by conventional metallurgical methods. The electrodes were polished to a mirror finish with SiC abrasive papers and diamond pastes down to a grain size of 0.5 μm and subsequently annealed in a butane flame and quenched in ultra-pure water according to the procedure reported in [25] for single-crystals and in [21] for polycrystals. The crystalline structure of the alloy electrodes was a disordered fcc solid solution.

SFG spectra were recorded in the following potential ranges: −1200 to +200 mV versus Ag/AgCl, spanned in steps of 200 mV, for Au electrodes and −1200 to −400 mV versus Ag/AgCl, spanned in steps of 200 mV, for Au–Cu and Au–Ag–Cu electrodes. The electrodes were immersed in the CN solution at open circuit and then polarised to the most cathodic potential, the potential was subsequently stepped in the positive direction. In order to check the presence of irreversible or hysteretic processes and to make sure than serial correlation among spectra is absent, a control spectrum was run at −1200 mV at the end of the positive-going potential staircase: the first spectrum and the last one overlapped perfectly.

The SFG setup used was analogous to the system described in [26]. Briefly, a flash-pumped YAG laser

produces 15 ps pulses with a 100 MHz repetition rate. These pulses form 1 μs long trains with a 25 Hz repetition rate. After amplification, the YAG pulses are used to pump two non linear crystals in parallel. The first one (BBO) receives 30% of the YAG pump to produce a green 532 nm laser beam through second harmonic generation. The remaining 70% pumps an $AgGaS_2$ crystal in an optical parametric oscillator which delivers a tunable infrared wavelength between 2.7 and 6.0 μm. The two laser beams are then spatially and temporally overlapped at the surface of the electrode to produce SFG and DFG. Both beams are p-polarized, with angles of incidence 55 and 65 degrees for the green and infrared beams, respectively. The energy resolution of the system was 2 cm^{-1}. The electrochemical setup allowed cyclic voltammetry and SFG/DFG experiments to be performed in the same cell which consisted of a Kel-F body, closed by a CaF_2 prism and filled with electrolyte, deaerated by Ar bubbling. Inside the cell, the electrode was fixed to a central stub and kept in contact with a gold wire by aspiration. A three-electrode configuration was used, with a platinum wire counter electrode and an Ag/AgCl reference electrode. For experimental purposes, the electrode was either gently pushed against the CaF_2 prism to carry out SFG/DFG measurements in a thin layer configuration or raised about 1 cm above the prism to perform cyclic voltammetry. A scan rate of 100 mV s^{-1} was employed. Values reported after the symbol ± refer to one standard deviation. Potentials are reported versus Ag/AgCl.

3 Results and discussion

3.1 Cyclic voltammetry

Details of the voltammetric behaviour of Au(111) and (210) in 0.1 M $NaClO_4$ in the absence and presence of KCN have been described elsewhere [27]. Similar work carried out with polycrystalline Au, Au–Cu and Au–Ag–Cu has also been reported [28]. In this section we do not repeat this information, but simply discuss the variations in the voltammetric behaviour brought about by the addition of 25 mM 4CP to the 0.1 M $NaClO_4$, 25 mM KCN solution.

The cyclic voltammograms for the Au single-crystal electrodes and Au and alloy polycrystalline electrodes are shown in Figs. 1 and 2, respectively. The addition of 4CP typically gives rise to higher c.d.s, and minor changes in the qualitative features of the voltammograms discussed in [27]. The higher c.d.s, which are recorded in all cases, with the exception of Au(210), can be explained in terms of the cathodic and anodic reactivity of 4CP under potential cycling discussed in [5, 6]. Notwithstanding the fairly well known reactivity of 4CP, no special voltammetric features

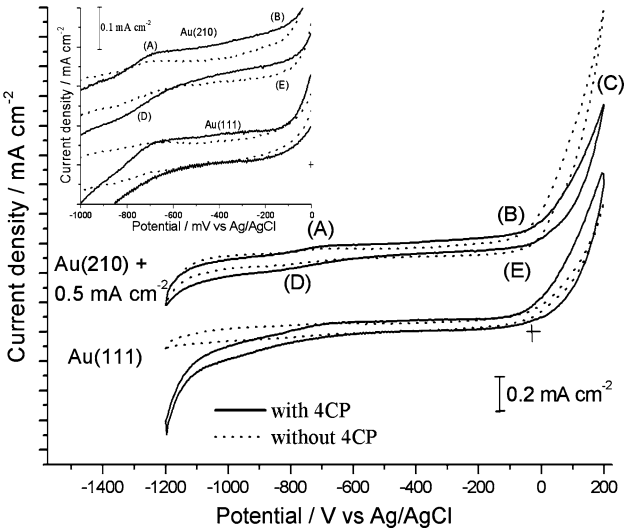

Fig. 1 Cyclic voltammetry of Au(111) and Au(210) electrodes in contact with a solution containing $NaClO_4$ 0.1 M, KCN 25 mM, with (solid lines) and without (dotted lines) 4-cyanopyridine 25 mM; scan rate 100 mV s^{-1}

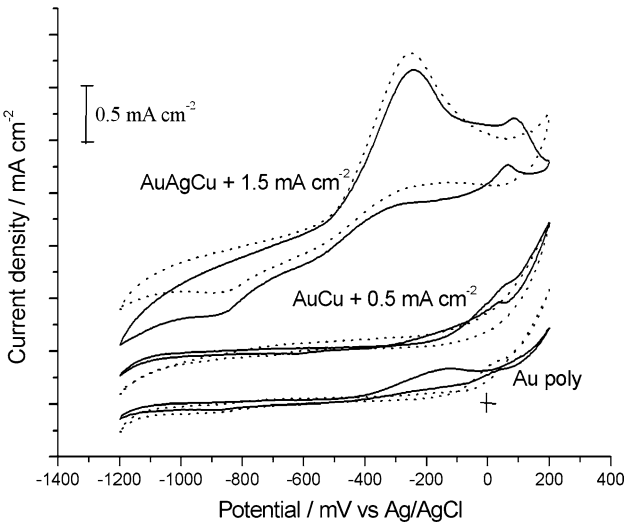

Fig. 2 Cyclic voltammetry of polycrystalline Au, Au–Cu and Au–Ag–Cu electrodes in contact with a solution containing $NaClO_4$ 0.1 M, KCN 25 mM, with (solid lines) and without (dotted lines) 4-cyanopyridine 25 mM; scan rate 100 mV s^{-1}

have been detected, with the exception of the c.d. crossover observed with poly-Au. In general, the following voltammetric changes are induced by the addition of 4CP. Peak (A) is shifted to more cathodic potentials; peak (B) is shifted to less cathodic potentials; peak (E) is either suppressed (Au(111)) or shifted to more cathodic values (poly-Au); peak (D) is shifted to less cathodic values. The shift of peak (A) to more anodic values suggests that CN^- adsorption is inhibited by the presence of 4CP, which is probably adsorbed onto Au° via the heteroaromatic N at potentials more cathodic than those required for CN^- adsorption.

The shift of peaks (B) and (E) to less anodic values hints at the fact that Au oxidation is favoured by the coadsorption of CN^- and 4CP, possibly owing to the enhanced electron-withdrawing activity of nitrile-bonded 4CP. The shift of peak (D) to less cathodic values indicates that the competition of 4CP, which possesses a stable cathodic adsorption configuration, favours the cathodic desorption of CN^-. This behaviour is more obvious with increasing packing of the Au faces. A marked change in the voltammetric behaviour of poly-Au is noticed upon addition of 4CP to the CN^--containing solution: peak (B) is remarkably depressed. This behaviour can be explained by the fact that coadsorbed 4CP alters the oxidation mode of poly-Au giving rise to suppression of the sites more prone to CN^--attack. The c.d. crossover observed in the anodic range might be explained by the decrease of the surface density of 4CP caused by the positive scan leading to consumption of surface 4CP. The more open face exhibits a lower activity towards both anodic and cathodic 4CP decomposition, while the more packed one displays an enhanced cathodic activity and a reduced anodic one. As observed in [23, 27], a more open face corresponds to enhanced metal–CN^- interaction. These conditions seem to correlate with a lower electrodic activity towards 4CP decomposition.

The voltammetric changes induced by the addition of 4CP in the Au–Cu system are similar to those observed with polycrystalline Au. In particular, by comparing the high anodic and high cathodic portions of the voltammograms, it is seen that the Au–Cu alloy exhibits the same features of compact Au single-crystal faces (see also [27]), in terms of enhanced cathodic and depressed anodic reactivity towards 4CP. Addition of 4CP to the Au–Ag–Cu system gives rise to the following characteristics: (i) the reactivity of 4CP seems to be depressed, much like the case of open Au single-crystal faces; (ii) the anodic peak at −250 mV is basically unaffected, while (iii) the one at +100 mV is, and its counterpart on the return scan is suppressed; (iv) a reduction peak at ca. 0 mV appears instead of that at ca. −100 mV noticed in the absence of 4CP, while the positions of the cathodic peaks at ca. −600 mV and −850 mV are not measurably affected by the addition of 4CP. Along the lines of the comments reported above, we can suggest that the behaviour of the Au–Ag–Cu alloy in the CN^- + 4CP electrolyte exhibits the principal features of open Au single-crystal faces: a reduced activity towards 4CP decomposition, probably induced by a higher stability of adsorbed CN^-. This suggestion is coherent with our analysis of the voltammetric behaviour at the relevant Au alloys in the pure supporting electrolyte [28].

3.2 In situ SFG and DFG spectroscopies

The potential-dependent SFG and DFG spectra at Au(111), Au(210) and polycrystalline Au, Au–Cu and Au–Ag–Cu electrodes in contact with solutions containing KCN and 4CP were measured. For the sake of brevity only the SFG and DFG spectra at Au(111) and Au–Cu are shown (Figs. 3, 4). It is seen that one CN stretching band appears, located in a range typical of adsorbed CN^-. No bands

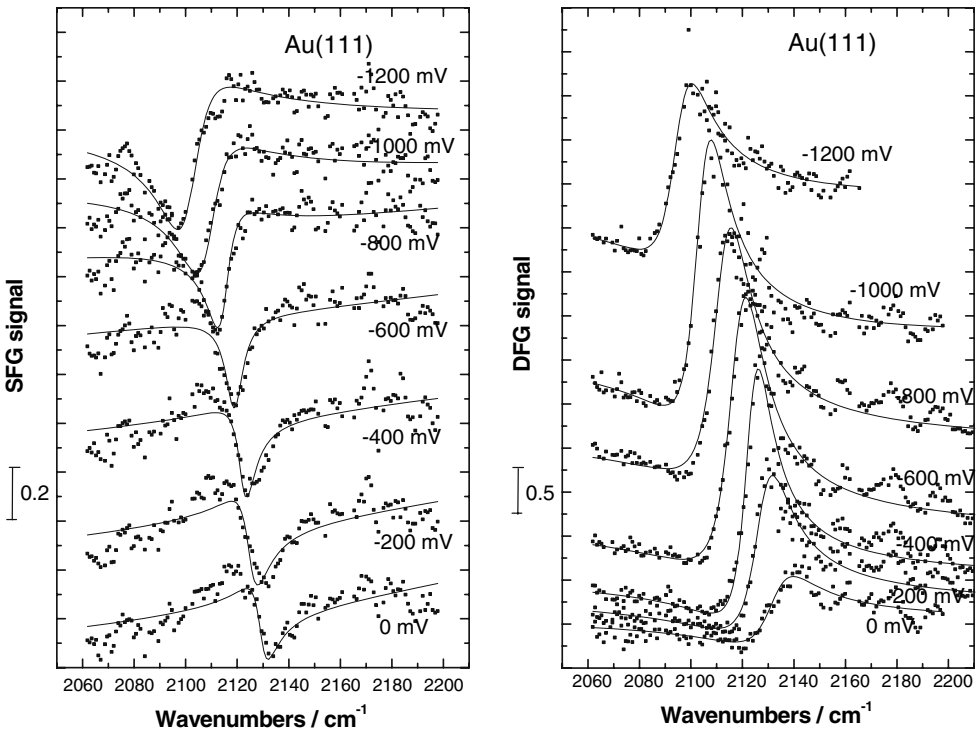

Fig. 3 Potential-dependent SFG and DFG spectra (squares) and results of the fit with the $|\chi^{(2)}|^2$ model (continuous line) for a Au(111) electrode in contact with a $NaClO_4$ 0.1 M, KCN 25 mM, 4-cyanopyridine 25 mM solution

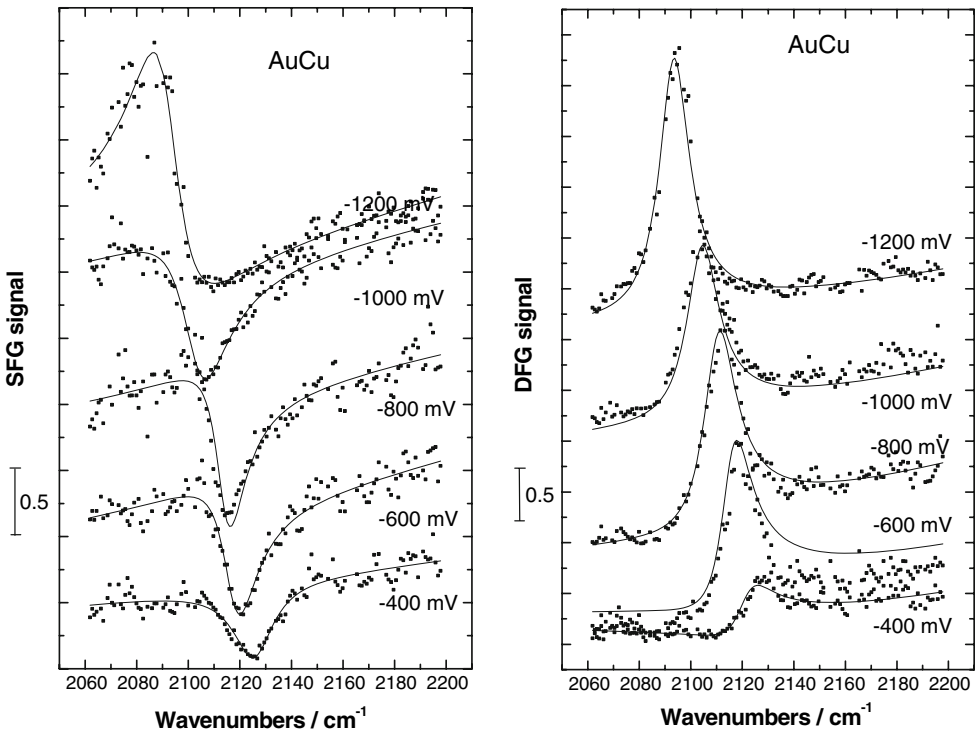

Fig. 4 Potential-dependent SFG and DFG spectra (squares) and results of the fit with the $|\chi^{(2)}|^2$ model (continuous line) for a polycrystalline Au–Cu electrode in contact with a $NaClO_4$ 0.1 M, KCN 25 mM, 4-cyanopyridine 25 mM solution

appear in the nitrile stretching region (2245 cm^{-1} for 4CP). From this it can be inferred that 4CP is not in direct contact with the electrode surface.

Elaborating on [4, 29–33], these spectra have been analysed quantitatively with the following model:

$I_{SFG/DFG} \propto |\chi^{(2)}|^2$ with

$$\chi^{(2)} = \chi^{(2)}_{ads} + \chi^{(2)}_{met} = \frac{A(V)}{\nu_{IR} - \nu_0(V) \pm i\Gamma_{SFG/DFG}} + a + i \cdot b$$

where:

(i) $\chi^{(2)}$ is the second-order surface susceptibility. It comprises two contributions to the SFG signal: $\chi^{(2)}_{ads}$is the resonant part arising from the adsorbates, whereas $\chi^{(2)}_{met}$ is the part due to the metallic substrate; the electrode contribution has been customarily regarded as non-resonant (e.g. [29]), but in this paper, dealing with Au-base alloys, we adopt a more general approach (see point (vi) below).

(ii) A is the resonator intensity, a function of potential V and coverage degree with CN^- θ. The potential dependence of A derives from the potential dependence of the quantities $\rho_a(E_F)$, α_V, α_e and U [31], where: $\rho_a(E_f)$ is the density of states at the Fermi level E_f of the adsorbate orbital involved in the dynamic coupling phenomenon; α_v and α_e are the vibrational and electronic parts of the molecular polarisability of the molecule undergoing adsorption; U is a term accounting for local field effects on the induced dipole of the adsorbate;

(iii) ν_{IR} is the scanned IR frequency;

(iv) $\nu_o(V) \cong \nu_{free} + a_2 + b_2V + c_2V^2$ is the potential-dependent resonant frequency, ν_{free} is the singleton frequency, a_2 and b_2 account for the potential dependence of $\rho_a(E_F)$, U, α_V, α_e and θ [23];

(v) $\Gamma_{SFG/DFG}$ is the resonator broadening;

(vi) a and b are the model constants, relating to the free-electron (a) and bound-electron "b" contributions to non-resonant term; "a" is essentially related to the surface charge density, while "b" is proportional to the population of bound electronic states with energy $h(\nu_{VIS} \pm \nu_{IR})$ (for details, see [29, 31]). The model adopted for $\chi^{(2)}_{met}$ is based on the harmonic oscillator approach [29, 34]. This electronic structure model, though commonly applied to single crystals of a pure metal, hardly contains crystallographic structure information and can thus be used for alloy and/or polycrystalline electrodes, provided correct values of the model parameters are identified. Since the frequency of the visible beams (exciting laser, SFG and DFG) is expected to be close to the interband resonance, this can be approximately accounted with a Lorentzian frequency dependence: $\chi^{(2)}_{met} = a + i \cdot b = \frac{A_{met}}{\nu_{VIS} - \nu_{0,met} \pm i\Gamma_{met}}$, where A_{met} is the electronic resonator intensity, $\nu_{o,met}$ is the electronic resonant frequency and Γ_{met} is the electronic resonator broadening. In the present investigation—in order to avoid numerical instabilities in the non-linear least-square (NLLS) fitting procedure, related to the

functional form of the model and to the number of model parameters, we shall keep the traditional symbols a and b for the parameters of $\chi^{(2)}_{met}$, but enhancement effects can result from electronic resonance.

Interference effects can be quantified in terms of the contrast parameter c proposed in [30]:

$$c = 2 \cdot |\chi^{(2)}_r| \cdot |\chi^{(2)}_{nr}| / \left[|\chi^{(2)}_r| 2 + |\chi^{(2)}_{nr}|^2 \right].$$

The fit parameters were identified as a function of potential with a minimisation procedure based on the Levemberg–Marquart algorithm.

3.2.1 Single-crystal and polycrystalline Au electrodes

Peak position of the vibrational resonance v_o. The potential-dependent resonance position v_o is shown in Fig. 5; cognate measurements carried in the absence of 4CP (see [27] for a more detailed report) and with polycrystalline Au (see [28]) are also reported, for the sake of comparison. No measurable differences were detected between SFG and DFG, the data are consequently pooled. In the inset we show curves obtained by pooling all the single-crystal and polycrystal results in the absence and presence of 4CP. The Stark tuning exhibits a linear dependence $v_o = A + B \cdot V$. The NLLS parameters are reported in Table 1.

Immaterial differences emerge between the parameter estimates reported in Table 1 corresponding to the addition of 4CP, the single adsorption site scenario envisioned in [27] seems to hold in this case too (see also Sect. 2.1.2), addition of 4CP does not apparently change charge transfer between CN^- and Au surfaces, regardless of the surface orientation and presence of grain boundaries.

Table 1 Results of the linear fit of potential-dependent resonance position (SFG and DFG data for Au(111), Au(210) and polycrystalline Au pooled)

Electrolyte	A/cm^{-1}	B/V^{-1} cm^{-1}
Without 4CP	2133.3 ± 1.9	30.50 ± 2.02
2 mM 4CP	2132.8 ± 1.8	31.11 ± 2.30

Peak half-width of the vibrational resonance Γ. As far as the peak half-width Γ is concerned, no measurable differences are found between SFG and DFG spectra recorded at different potentials, the corresponding results are consequently pooled and shown in Fig. 6. In this plot we highlight the electrode types and the electrolyte composition. From this figure it can be concluded that no discernible effects are brought about by 4CP addition to the KCN solution upon varying the surface crystallographic structure and the potential within the double-layer charging region. This result confirms the view that a single adsorption site is available for CN^- on Au (see [27] and Sect. 2.1.1).

Normalised resonator strength A_N. The normalised resonator strength values A_N for single- and polycrystalline Au electrodes in contact with KCN solutions without and with 4CP are shown as a function of potential in Fig. 7. In these plots we pooled SFG and DFG results, since the corresponding estimates cannot be distinguished in a statistically significant way. The typical anodic decrease discussed in [27, 29] is also found in these experiments.

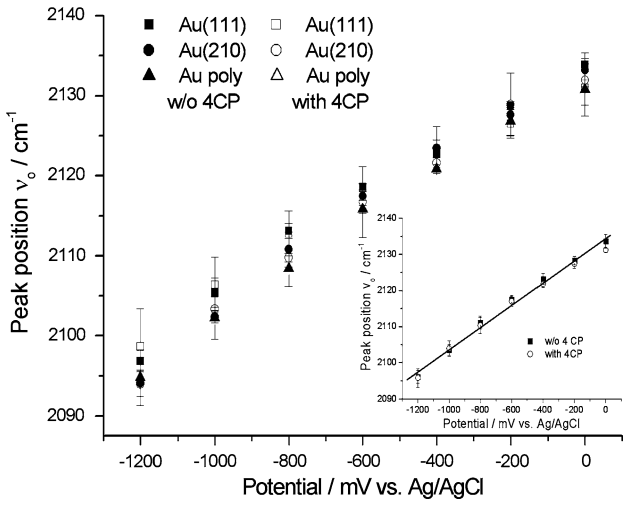

Fig. 5 Potential-dependent peak position v_o estimated from SFG and DFG spectra for Au(111), Au(210) and polycrystalline Au electrodes in contact with solutions of composition: 0.1 M $NaClO_4$, 25 mM KCN, without and with 4-cyanopyridine 25 mM. Inset: same as above, but with data from the three electrodes pooled

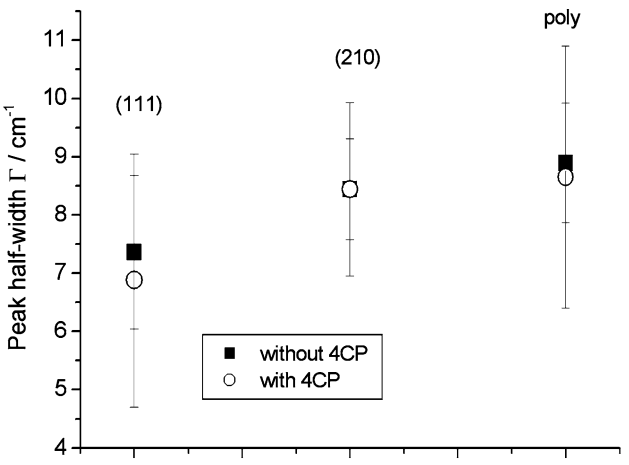

Fig. 6 Peak half-width Γ estimated from SFG and DFG spectra measured at the potentials in the range −1.2 to 0.0 V versus Ag/AgCl for Au(111), Au(210) and polycrystalline Au electrodes in contact with solutions of composition: 0.1 M $NaClO_4$, 25 mM KCN, without and with 4-cyanopyridine 25 mM

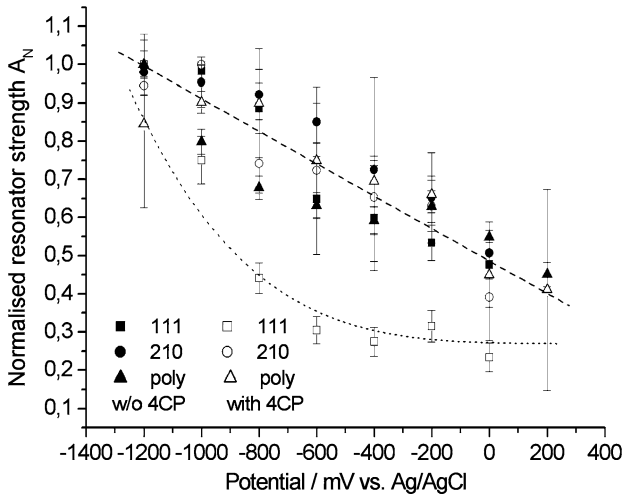

Fig. 7 Potential-dependent normalised resonator strength A_N estimated from SFG and DFG spectra for Au(111), Au(210) and polycrystalline Au electrodes in contact with solutions of composition: 0.1 M $NaClO_4$, 25 mM KCN, without and with 4-cyanopyridine 25 mM

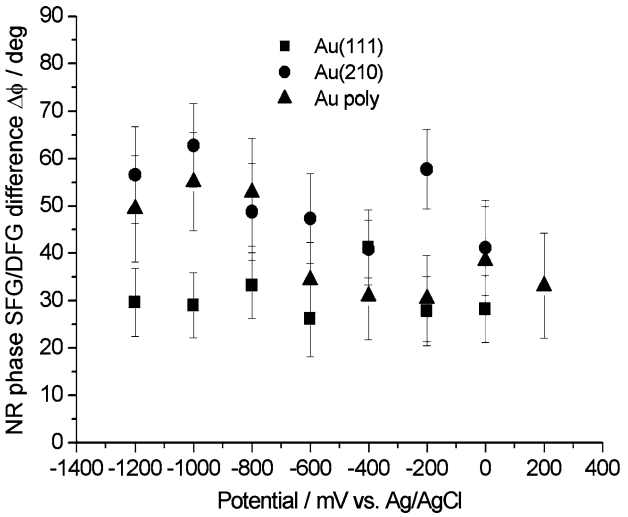

Fig. 8 Potential-dependent differences between the phases of the non-resonant contribution to the second-order susceptibility measured by SFG and DFG $\Delta\phi_{NR}$ estimated from SFG and DFG spectra for Au(111), Au(210) and polycrystalline Au electrodes in contact with a solution of composition: 0.1 M $NaClO_4$, 25 mM KCN, 2 mM 4-cyanopyridine

Quantitative effects of 4CP addition emerge only for Au(111). A similar effect was noticed for cetylpyridinium chloride [23]: closely-packed surfaces, such as (111) for fcc Au, are affected (i.e. the desorption rate is increased), while loosely packed—such as (210)—and defective ones–such as that of a polycrystal—exhibit the same desorption rate as in the absence of the additive. This result might be related to the fact that the additive tends to reduce the coupling among adsorbates, thus lowering their repulsive interactions.

Difference between the phases of the non-resonant term of SFG and DFG spectra $\Delta\phi_{NR}$. In Fig. 8 we report the difference between the phases of the non-resonant terms estimated from SFG and DFG spectra as a function of potential. In [27] we showed that $\Delta\phi_{NR}$ exhibits a potential dependence that seems to be absent when 4CP is added. If the results measured at the different potentials are pooled, the following results are obtained: (111) 30.7 ± 5.1°, (210) 50.8 ± 8.5°, polycrystal 40.6 ± 10.2°. Limited quantitative differences are found, suggesting that Au(111) has a different behaviour with respect to the other surfaces: this behaviour can be related to the effects of 4CP found on A_N and could be the electronic-structure counterpart of the variations of lateral interactions among adsorbed CN^- ions brought about by the presence of the additive with the most densely packed surface.

Contrast parameter c. As far as the interaction between the electronic vibrational structures are concerned, we also evaluated the contrast function at resonance $c(\nu_o)$: our results show no statistically significant differences between the experiments carried out in the absence and presence of 4CP. The comments relevant to the 4CP-free case, already reported in [27], also apply for the present case.

3.2.2 Au-alloy electrodes

Peak position of the vibrational resonance ν_o. The estimates of the potential-dependent vibrational resonance ν_o for polycrystalline Au, Au–Cu and Au–Ag–Cu alloys are shown in Fig. 9. SFG and DFG data are pooled for the

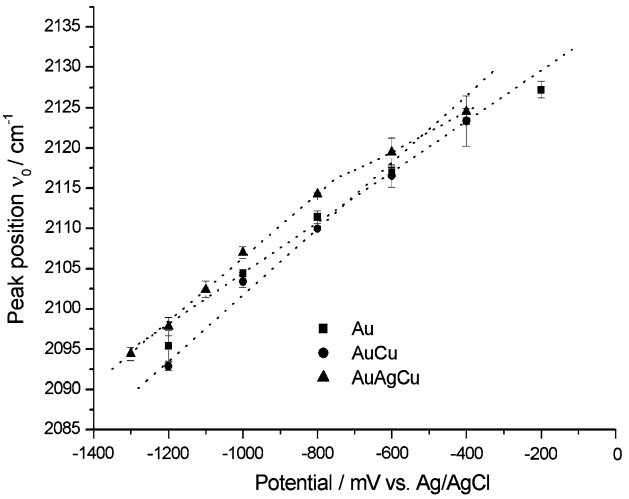

Fig. 9 Potential-dependent peak position ν_o estimated from SFG and DFG spectra for polycrystalline Au, Au–Cu and Au–Ag–Cu electrodes in contact with solutions of composition: 0.1 M $NaClO_4$, 25 mM KCN, without and with 4-cyanopyridine 25 mM

Table 2 Results of the linear fit of the potential-dependent resonance position for polycrystalline Au, Au–Cu and Au–Ag–Cu (SFG and DFG data pooled). In the experiments with Au–Ag–Cu, /1/ and /2/ refer to the potential intervals −1.2 to −0.7 V versus Ag/AgCl and −0.7 to −0.3 V versus Ag/AgCl, respectively

System	A/cm^{-1}	B/V^{-1} cm^{-1}
Au without 4CP	2133.0 ± 0.9	29.35 ± 1.84
Au–Cu without 4CP	2136.2 ± 1.1	34.27 ± 1.24
Au–Ag–Cu without 4CP/1/	2144.9 ± 0.3	37.87 ± 3.30
Au–Ag–Cu without 4CP/2/	2131.0 ± 1.9	19.23 ± 3.26
Au with 4CP	2134.4 ± 0.2	31.46 ± 0.30
Au–Cu with 4CP	2142.9 ± 1.7	41.27 ± 0.21
Au–Ag–Cu with 4CP/1/	2146.0 ± 0.7	39.56 ± 3.83
Au–Ag–Cu with 4CP/2/	2134.8 ± 0.1	25.77 ± 0.64

reasons given in Sect. 2.1.1. In this set of experiments the Stark tuning exhibits a linear dependence $\nu_o = A + B \cdot V$, with Au–Ag–Cu alloys a slope discontinuity can be observed at ca. −0.7 V, corresponding to the corrosion potential (see Fig. 2). The NLLS parameters are reported in Table 2. Results corresponding to the 4CP-free electrolyte (see [27] for details) are also reported for comparison.

Regardless of the presence of 4CP, the Stark shift values are found to rank as follows: Au–Ag–Cu (anodic range)<Au<Au–Cu ≅ Au–Ag–Cu (cathodic range). Addition of 4CP corresponds to an increase of the Tafel slopes measured with Au–Cu electrodes and the Au–Ag–Cu surface in the anodic range.

Peak half-width of the vibrational resonance Γ. Γ values found by NLLS for polycrystalline Au, Au–Cu and Au–Ag–Cu alloy electrodes in contact with KCN solutions in the absence (for a further discussion, see [28]) and in the presence of 4CP are shown in Fig. 10. Results from SFG and DFG experiments do not exhibit statistically significant differences and are pooled. Addition of 4CP quenches the variation of Γ with potential found at anodic potentials. This kind of behaviour might be related to the corrosion-inhibiting action of this substance proved for Ag [12] and can be described in terms of a reduction of the multiplicity of kinds of adsorption sites made available by the corrosion process.

Normalised resonator strength A_N. The potential-dependent estimates of A_N for polycrystalline Au, Au–Cu and Au–Ag–Cu in the absence (see [28] for a detailed presentation) and in the presence of 4CP are reported in Fig. 11. No measurable differences appear between experiments without and with 4CP, this result is in keeping with that of [27] that 4CP effects on A_N can be found only with the Au(111) surface that maximises the lateral interaction among adsorbed CN^-.

Difference between the phases of the non-resonant term of SFG and DFG spectra $\Delta\phi_{NR}$. The differences $\Delta\phi_{NR}$

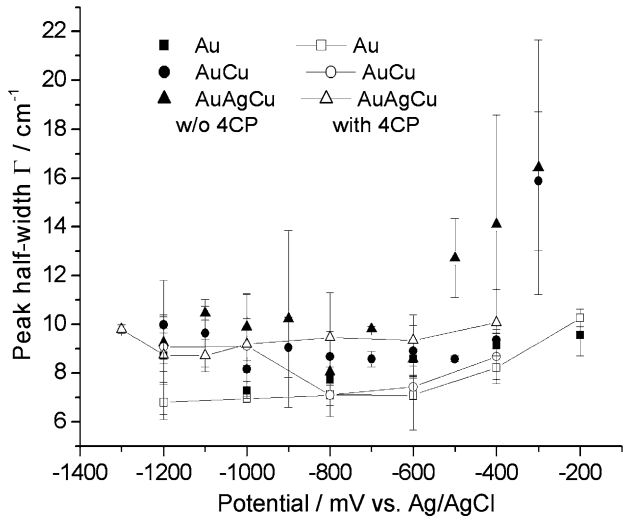

Fig. 10 Potential-dependent peak half-width Γ estimated from SFG and DFG spectra for polycrystalline Au, Au–Cu and Au–Ag–Cu electrodes in contact with solutions of composition: 0.1 M $NaClO_4$, 25 mM KCN, without and with 4-cyanopyridine 25 mM

between the phases of the non-resonant part of the second-order susceptibility are reported as a function of potential in Fig. 12. Remarkable effects of 4CP on the electronic structure of the metal substrates can be inferred. An analysis of these effects requires intensive physical modelling and is beyond the scope of the present work.

Contrast parameter c. We computed the contrast function at resonance $c(\nu_o)$ for the relevant systems and compared them with the results obtained for the corresponding 4CP-free systems, discussed elsewhere [28]. The addition of 4CP brings about differences with alloy

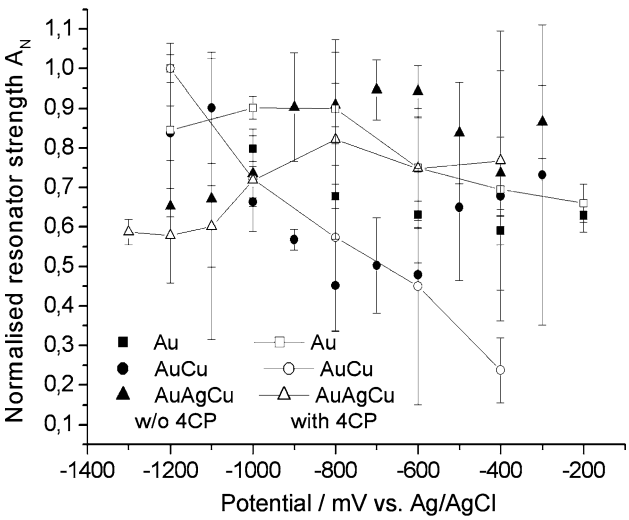

Fig. 11 Potential-dependent normalised resonator strength A_N estimated from SFG and DFG spectra for polycrystalline Au, Au–Cu and Au–Ag–Cu electrodes in contact with solutions of composition: 0.1 M $NaClO_4$, 25 mM KCN, without and with 4-cyanopyridine 25 mM

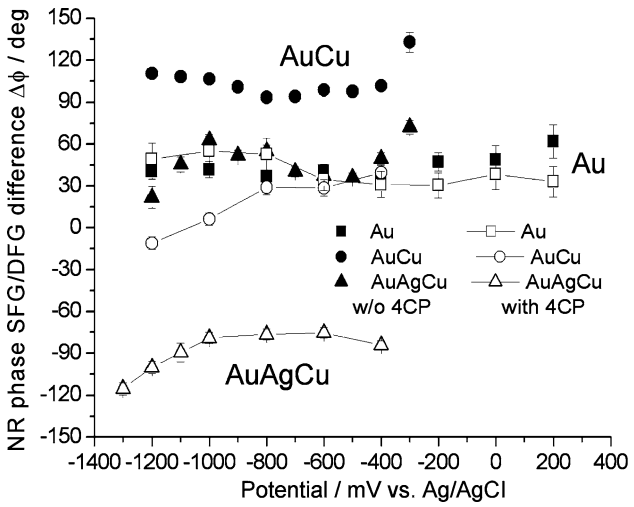

Fig. 12 Potential-dependent differences between the phases of the non-resonant contribution to the second-order susceptibility measured by SFG and DFG $\Delta\phi_{NR}$ estimated from SFG and DFG spectra for polycrystalline Au, Au–Cu and Au–Ag–Cu electrodes in contact with solutions of composition: 0.1 M $NaClO_4$, 25 mM KCN, without and with 4-cyanopyridine 25 mM

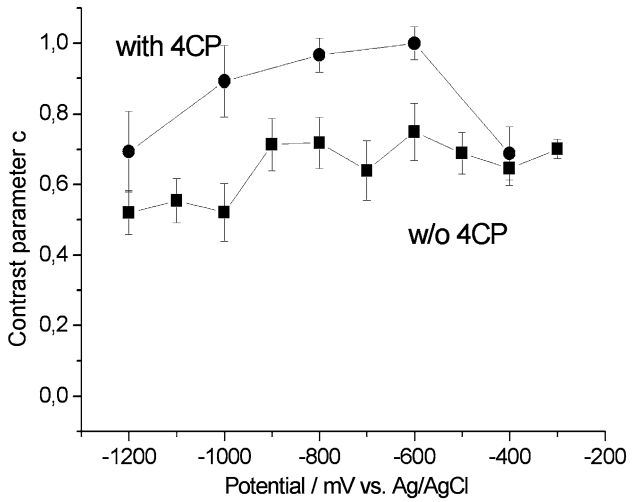

Fig. 13 Potential-dependent contrast parameter *c* estimated from DFG spectra for a polycrystalline Au–Cu electrode in contact with solutions of composition: 0.1 M $NaClO_4$, 25 mM KCN, without and with 4-cyanopyridine 25 mM

electrodes. The most marked differences are obtained with Au–Cu by DFG and are reported in Fig. 13. The rationalisation of these results awaits suitable physical modelling.

4 Conclusions

In this work we investigated the potential-dependent behaviour of Au(111), Au(210), polycrystalline Au, Au–Cu and Au–Ag–Cu electrodes in contact with aqueous solutions containing 4-cyanopyridine (4CP) and KCN. This study was performed by cyclic voltammetry and SFG/DFG in situ spectroscopies. We stressed the effects of 4CP additions to the CN^--containing solutions.

The voltammetric behaviour of CN^- at Au(hkl) and polycrystalline Au is affected by the addition of 4CP. In particular, peak shifts and peak suppressions are found, denoting variations of the adsorption potential range of CN^-. The differences among the investigated orientations can be explained with their respective degrees of atomic packing. Regarding the electrodic reactivity of 4CP, the more open faces exhibit a lower activity towards both anodic and cathodic decomposition, while the more packed ones display an enhanced cathodic activity and a reduced anodic one. Au–Cu exhibits a behaviour similar to that of polycrystalline Au. The Au–Ag–Cu system shows a reduced activity towards 4CP decomposition, probably induced by a higher stability of adsorbed CN^-.

We analysed the SFG and DFG spectra with a model accounting for the resonant and non-resonant contributions to the second-order interfacial susceptibility.

The Stark tuning of single- and polycrystalline Au is not affected by the addition of 4CP, while that of alloys tends to be increased. Stark tuning and resonance width results denote that a single adsorption site is present on Au, regardless of the atomic ordering of the surface and of the presence of 4CP. 4CP effects on the resonance width are compatible with the action of this substance as a corrosion inhibitor. This interpretation is corroborated by our non-resonant phase-difference results, in fact addition of 4CP quenches the potential dependence of this parameter related to the electronic structure of the electrode.

As far as the resonator strength is concerned, the only measurable effects are found with Au(111), suggesting that the additive causes a decrease of the lateral interactions among adsorbed CN^-.

Acknowledgements Highly qualified and continuous technical assistance by the SFG collaborators and CLIO staff, Bâtiment 209D, Centre Universitaire Paris Sud, 91405 Orsay, France, is gratefully acknowledged.

References

1. Yang DF, Lipkowski J (1995) Russian J Electrochem 31:768
2. Chen AC, Sun SG, Yang D, Pettinger B, Lipkowski J (1996) Can J Chem 74:2321
3. Chen AC, Yang D, Lipkowski J (1999) J Electroanal Chem 475:130
4. Pluchery O (2000) Thèse de doctorat. Université Paris XI
5. Pluchery O, Tadjeddine A (2001) J Electroanal Chem 500:379
6. Pluchery O, Climent V, Rodes A, Tadjeddine A (2001) Electrochim Acta 46:4319
7. Furukawa H, Takahashi M, Ito M (1986) Chem Phys Lett 132:498
8. Rubim JC (1987) J Electroanal Chem 220:339

9. Shi C, Zhang W, Birke RL, Lombardi JR (1997) J Electroanal Chem 423:67
10. Bozzini B, Fanigliulo A, Mele C (2003) Trans IMF 81:59
11. Bozzini B, Cavallotti PL, Fanigliulo A, Giovannelli G, Mele C, Natali S (2004) J Solid State Electrochem 8:147
12. Bozzini B, Giovannelli G, Mele C, Brunella F, Goidanich S, Pedeferri P (2006) Corros Sci 48:193
13. Bozzini B, D'Urzo L, Mele C A SERS investigation of the electrodeposition of Cu from acidic sulphate solutions in the presence of 4-cyanopyridine (In preparation)
14. Ohtani M, Sunagawa T, Kuwabata S, Yoneyama H (1997) J Electroanal Chem 429:75
15. Huerta F, Morallón E, Vázquez JL (1999) Surf Sci 431:L577
16. Huerta F, Morallón E, Cases F, Rodes A, Vázquez JL, Aldaz A (1997) J Electroanal Chem 421:179
17. Huerta F, Morallón E, Vázquez JL, Aldaz A (1997) J Electroanal Chem 431:269
18. Huerta F, Morallón E, Cases F, Rodes A, Vázquez JL, Aldaz A (1998) J Electroanal Chem 445:155
19. Huerta F, Morallón E, Vázquez JL, Aldaz A (1999) J Electroanal Chem 475:38
20. Zhen C-H, Sun S-G, Fan C-J, Chen S-P, Mao B-W, Fan Y-J (2004) Electrochim Acta 49:1249
21. Huerta F, Mele C, Bozzini B, Mórallon E (2004) J Electroanal Chem 569:53
22. Fanigliulo A, Bozzini B (2002) J Electroanal Chem 530:53
23. Bozzini B, Mele C, Fanigliulo A, Busson B, Vidal F, Tadjeddine A (2004) J Electroanal Chem 574:85
24. Bozzini B, Mele C, Tadjeddine A (2004) J Cryst. Growth 271:274
25. Hamelin A, Katayama A (1981) J Electroanal Chem 117:221
26. Mani AA, Dreesen L, Hollander Ph, Humbert C, Caudano Y, Thiry PA, Peremans A (2001) Appl Phys Lett 79:1945
27. Bozzini B, Busson B, De Gaudenzi GP, Mele C, Tadjeddine A (2008) J Solid State Electrochem 12:303
28. Bozzini B, Busson B, De Gaudenzi GP, Mele C, Tadjeddine A (2007) J Alloys Compd 427:341
29. Tadjeddine A, Le Rille A (1999) In: Wieckowski A (ed) Interfacial electrochemistry. Dekker, NY, p 317
30. Le Rille A (1997) Thèse de doctorat. Université de Paris-sud
31. Vidal F (2003) Thèse de doctorat. Université Paris XI
32. Hayashi M, Lin SH, Raschke MB, Shen YR (2002) J Phys Chem A 106:2271
33. Raschke MB, Hayashi M, Lin SH, Shen YR (2002) Chem Phys Lett 359:367
34. Pauli W (2000) Optics and the theory of electrons. Dover Publications Inc., New York